The Astrophysical Journal Letters, 754:L36 (6pp), 2012 August 1 doi:10.1088/2041-8205/754/2/L36

ON THE FORMATION OF HOT JUPITERS IN STELLAR BINARIES

Smadar Naoz[1,2], Will M. Farr[2], and Frederic A. Rasio[2,3]
[1] Harvard Smithsonian Center for Astrophysics, Institute for Theory and Computation, 60 Garden Street, Cambridge, MA 02138, USA
[2] Center for Interdisciplinary Exploration and Research in Astrophysics (CIERA), Northwestern University, Evanston, IL 60208, USA
[3] Department of Physics and Astronomy, Northwestern University, Evanston, IL 60208, USA
Received 2012 June 8; accepted 2012 July 2; published 2012 July 17

ABSTRACT

We study the production of hot Jupiters (HJs) in stellar binaries. We show that the "eccentric Kozai–Lidov" (EKL) mechanism can play a key role in the dynamical evolution of a star–planet–star triple system. We run a large set of Monte Carlo simulations including the secular evolution of the orbits, general relativistic precession, and tides, and we determine the semimajor axis, eccentricity, inclination, and spin–orbit angle distributions of the HJs that are produced. We explore the effect of different tidal friction parameters on the results. We find that the efficiency of forming HJs when taking the EKL mechanism into account is higher then previously estimated. Accounting for the frequency of stellar binaries, we find that this production mechanism can account for about 30% of the observed HJ population. Current observations of spin–orbit angles are consistent with this mechanism producing ∼30% of all HJs, and up to 100% of the misaligned systems. Based on the properties of binaries without an HJ in our simulations, we predict the existence of many Jupiter-like planets with moderately eccentric and inclined orbits and semimajor axes of several AU.

Key words: binaries: general – planetary systems

Online-only material: color figures

1. INTRODUCTION

At least ∼20% of exoplanets are associated with one or more stellar companions (Raghavan et al. 2006; Desidera & Barbieri 2007; Eggenberger et al. 2007; Mugrauer & Neuhäuser 2009; Raghavan et al. 2010). Stellar companions may significantly alter the planetary orbits around their partner on secular timescales. Close-in giant planets tend to be found preferentially in binary stellar systems (Zucker & Mazeh 2002; Udry & Santos 2007). On the other hand, recent studies suggest that the frequency of giant planets in close binaries (<100 AU) is significantly lower than in the overall population (e.g., Eggenberger et al. 2011), indicating that distant stellar perturbers may be important in the production of hot Jupiter (HJs).

Recent measurements of the sky-projected angle between the orbits of several HJs and the spins of their host stars have shown that misalignment and even retrograde orbits are common (e.g., Triaud et al. 2010; Albrecht et al. 2012). If these planets migrated in from much larger distances through their interaction with the protoplanetary disk (Lin & Papaloizou 1986; Masset & Papaloizou 2003), their orbits should have low eccentricities and inclinations (but see Lai et al. 2011; Thies et al. 2011). An alternative scenario that can account for the retrograde orbits involves the secular interaction between a planet and a binary stellar companion (Wu & Murray 2003; Fabrycky & Tremaine 2007; Wu et al. 2007; Takeda et al. 2008; Correia et al. 2011).

Many theoretical studies have investigated the role of secular perturbations in triple systems (Holman et al. 1997; Wu & Murray 2003; Fabrycky & Tremaine 2007; Wu et al. 2007; Takeda et al. 2008; Correia et al. 2011; Naoz et al. 2011a, 2011b; Veras & Tout 2012; Kratter & Perets 2012). Long-term stability requires that the system be sufficiently hierarchical. For an inner binary (stellar mass m_1 and planet mass m_2) in a nearly-Keplerian orbit with semimajor axis (SMA) a_1, the outer orbit for mass m_3 around the center of mass of the inner binary must have SMA $a_2 \gg a_1$. For stability, the eccentricity of the outer orbit, e_2, must also be small enough for m_3 to avoid close approaches with the inner orbit. In such systems, a sufficiently inclined m_3 can produce large-amplitude oscillations of the eccentricities and inclinations of the m_1–m_2 system, while a_1 and a_2 remain nearly constant; this is the so-called Kozai–Lidov mechanism (Kozai 1962; Lidov 1962).

The standard treatment (Kozai 1962) assumes that $m_2 \ll m_1$, m_3, and $e_2 \simeq 0$. Recently, Naoz et al. (2011a, 2011b) showed that these approximations are not appropriate for many systems. In the presence of an eccentric outer orbit, or if the test particle approximation for the inner planet is relaxed, the behavior of the system can be qualitatively different. The different behavior is associated with breaking of the axial symmetry present in the standard Kozai analysis; the associated lack of conservation of the axial component of the inner orbit's angular momentum allows the orbit to reach extremely high eccentricities and can even "flip" the orbit from prograde to retrograde (with respect to the total angular momentum).

Here, we study the evolution of Jupiter-like planets in binaries through Monte Carlo simulations. We include an octupole-level approximation to the perturbing potential and the tidal interactions between the star and the planet (following Eggleton & Kiseleva-Eggleton 2001), as well as general relativistic precession.

2. NUMERICAL SETUP

We set $m_1 = 1\,M_\odot$, $m_2 = 1\,M_J$, and $m_3 = 1\,M_\odot$ for all our calculations. We denote the inclination angle of the inner (outer) orbit with respect to the total angular momentum by i_1 (i_2), so that the mutual inclination between the two orbits is $i_{\rm tot} = i_1 + i_2$. We call the angle between the spin of the inner star and the direction of the angular momentum of the inner orbit ψ. The projection of ψ onto the plane of the sky, λ, can be observed through the Rossiter–McLaughlin effect (e.g., Gaudi & Winn 2007) and other methods (e.g., Nutzman et al. 2011; Sanchis-Ojeda & Winn 2011; Shporer et al. 2012).

Table 1
Parameters of the Monte Carlo Simulations

Name	a_2 (AU)	e_1 (initial)	$t_{V,2}$ (yr)	HJs %	$\psi > 90^\circ$ %	Total Runs
SMA1000	100	0.01	1.5	13	50	2478
SMA100	1000	0.01	1.5	1	60	3165
SMA500	500	0.01	1.5	19	44	2130
SMA500L	500	0.01	0.015	18	46	2014
SMA500H	500	0.01	150	0.5	25	2514
SMARan	Uniform in log	0.01	1.5	13	44	2424
SMARane1R	Uniform in log	Rayleigh	1.5	10	39	1674

Notes. In all runs, we start the Jupiter in a circular orbit at 5 AU. The arguments of periastron, g_1 and g_2, were chosen from a uniform distribution, and the mutual inclination between the inner and outer orbits is drawn isotropically. On a few days orbit, $t_V = 1.5$ yr is equivalent to $Q \simeq 2 \times 10^5$ while $t_V = 0.015$ yr and $t_V = 150$ yr (used in the SMA500L and SMA500H runs) are equivalent to $Q \simeq 2 \times 10^3$ and 2×10^7, respectively. For the star, we choose $t_V = 50$ yr in all runs, which is equivalent to $Q \simeq 10^5$.

We solve the octupole-level secular equations numerically following Naoz et al. (2011b). We are able to follow the spin vectors of both the planet and the star (which are set initially to 25 days and 10 days, respectively). The effects of tides and spins agree with those of Fabrycky & Tremaine (2007) and Eggleton & Kiseleva-Eggleton (2001). In many of our simulations, the inner orbit reaches extremely high eccentricities. During excursions to high eccentricity, there is a competition between the increased efficiency of tides leading to the Kozai capture process (Naoz et al. 2011a) and the possibility of destroying the system by crossing the Roche limit.

The upper limit for each system's integration time in all our simulations was 9 Gyr. However, if the planet becomes tidally captured by the inner star, the integration becomes extremely expensive. We therefore stop the simulation, classifying the planet as an HJ, whenever $a_1 < 0.03$ AU and $e_1 < 0.01$, or $a_1 < 0.06$ AU and $e_1 < 0.4$. These conditions imply either a circular HJ or an eccentric one, respectively. If a planet crosses the Roche limit, then we also stop the run and we consider it lost (see below).

We draw outer periods from the log-normal distribution of Duquennoy & Mayor (1991), but require that the corresponding a_2 lies between 51 and 1500 AU. At these separations, the distribution is approximately constant in $\log(P_2)$, where P_2 is the outer orbit period. The distribution of the outer eccentricity is assumed thermal.[4] We also performed runs for which we fix $a_2 = 100$, 500, or 1000 AU. These runs serve as a "zoom-in" since they give slices through the larger SMA parameter space. Two additional runs have different tidal friction parameters, varied over two orders of magnitude. Motivated by Moorhead et al. (2011), we adopt a Rayleigh distribution for e_1 with a mean eccentricity of 0.175 for one of the runs. All runs are summarized in Table 1. Note that all our initial conditions are stable according to the Mardling & Aarseth (2001) criterion.

The differential equations that govern the inner binary's tidal evolution were presented in Eggleton & Kiseleva-Eggleton (2001). These equations take into account stellar distortion due to tides and rotation, with tidal dissipation based on the theory of Eggleton et al. (1998). The viscous timescale, t_V, is related to the quality factor Q (Goldreich & Soter 1966) by

$$Q = \frac{4}{3}\frac{k_L}{(1+2k_L)^2}\frac{Gm}{R^3}\frac{t_V}{n}, \quad (1)$$

where $n = 2\pi/P$ is the mean motion of the orbit and k_L is the classical apsidal motion constant. We use the typical value $k_L = 0.014$, valid for $n = 3$ polytropes, when representing stars and $k_L = 0.25$, valid for $n = 1$ polytropes, when representing gas giant planets (Eggleton & Kiseleva-Eggleton 2001; Fabrycky & Tremaine 2007). Table 1 specifies the different viscous times we have used in our treatment for the Jupiter-like planet.

The eccentric Kozai–Lidov (EKL) mechanism can cause evolution of e_1 to extremely high values, implying a high probability that a planet will cross the Roche limit. Following Matsumura et al. (2010), we define

$$R_L = \frac{R_2}{0.6}\left(\frac{m_2}{m_2+m_1}\right)^{-1/3}, \quad (2)$$

where $R_2 = 1\,R_J$. If we find that $a_1(1-e_1) < R_L$, we stop the run and assume that the planet is lost.

3. RESULTS

In Figure 1, we show the fraction of systems that have survived the EKL mechanism as a function of SMA (for both the SMARan and SMARane1R runs), and as a function of the outer orbit eccentricity in the "zoom-in" runs. In these figures, we also show the fraction of systems that formed HJs via the Kozai capture mechanism. For wide separations ($a_2 > 100$ AU), the EKL mechanism and Kozai capture are far more efficient than suggested previously (Wu et al. 2007; Fabrycky & Tremaine 2007). In Figure 1, top right panel, we also compare our results to those of Naoz et al. (2011a) for a planetary perturber.

In Figure 2, we show the initial conditions that are associated with HJ formation. Most of the systems that form HJs lie within the bounds of an analytic criterion for determining the regions of parameter space associated with flipping the inner orbit in the test particle approximation (Lithwick & Naoz 2011; Katz et al. 2011). Before the flip occurs, the inner orbit's eccentricity becomes extremely high, often resulting in Kozai capture. Overall, the EKL mechanism and Kozai capture produce HJs about 15% of the time for the systems we considered.

In Figure 3, we show the distribution of mutual inclination, $i_{\rm tot}$, and spin–orbit angle, ψ, resulting from our simulations. Consideration of the octupole-level secular evolution when the inner body is a test particle (Katz et al. 2011) shows that the average part of the octupole Hamiltonian peaks for minimum inner eccentricity of $\simeq$0.335 and inclination $i_{\rm tot} \simeq 61.^\circ7$. This may be related to the peak observed in Figure 3 around 60°. An identical peak occurs for the test particle octupolar Hamiltonian at the corresponding retrograde inclination of 120°. In this work, we find that the retrograde peak is wider, suggesting that retrograde orbits are more stable than prograde orbits (e.g., Innanen 1980; Morais & Giuppone 2012).

4. SPIN–ORBIT ANGLES AND COMPARISON WITH OBSERVATIONS

Any proposed mechanism for producing misaligned HJs should be consistent with both the observed *shape* of the

[4] Recently, Raghavan et al. (2010) showed that the eccentricity distribution for Sun-like stars is closer to uniform. Therefore, we have conducted an additional run similar to SMA500 but with the stellar–binary eccentricity drown from a uniform distribution. We have found that the results were essentially unaffected.

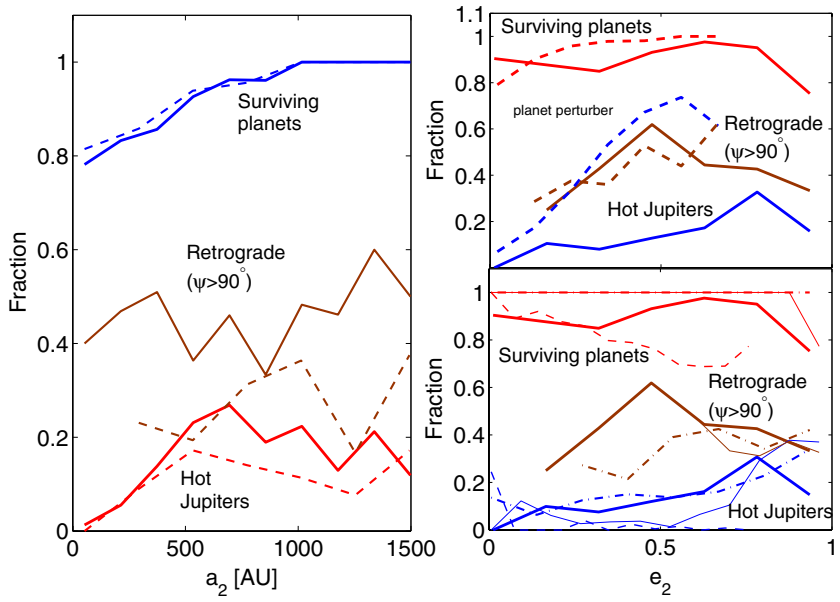

Figure 1. Fraction of planets as a function of outer SMA (left) and the outer orbit eccentricity (right). In the left panel, we consider the SMARan (solid lines) and SMARane1R (dashed lines) runs. We show the fraction of systems that survive the EKL process (blue lines), the fraction of systems that formed HJs via Kozai capture (red lines), and the fraction of HJs that ended up in retrograde motion with respect to the stellar spin axis ($\psi > 90^\circ$, brown lines). In the bottom right panel, we consider the SMA500 run (solid thick line), the SMA1000 run (solid thin line), the SMA100 run (thin dashed lines), and the run with extremely efficient tides, SMA500L (dot-dashed lines). The SMA500H run had extremely low efficiency of HJ formation and does not appear here. In the top right panel, we compare the SMA500 run (solid thick line) to a system in which the perturber is another giant planet (dashed lines) (Naoz et al. 2011a).

(A color version of this figure is available in the online journal.)

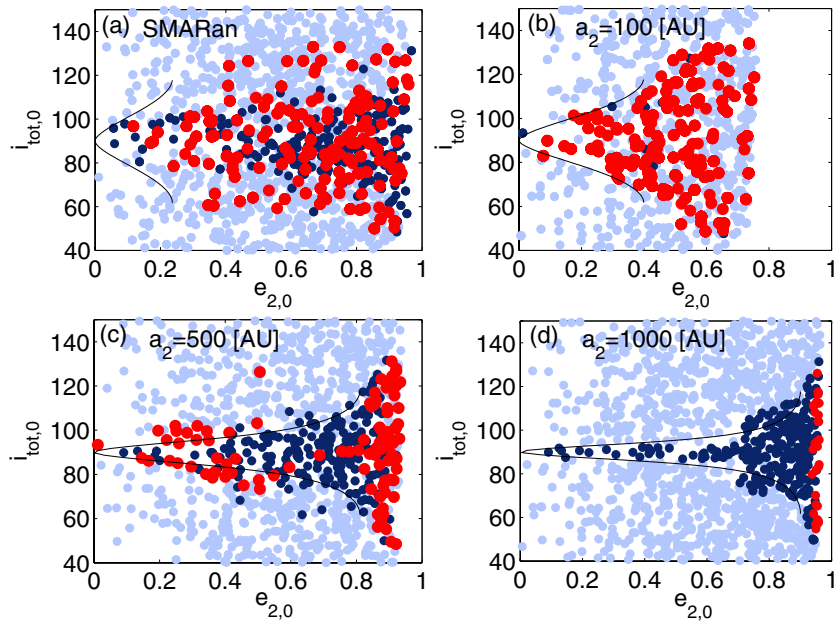

Figure 2. Formation of HJs as a function of initial conditions. We consider the initial mutual inclination, $i_{\rm tot,0}$, and the initial outer orbit eccentricity, $e_{2,0}$. The complete suite of runs are marked by the light blue dots. In dark blue, we mark the systems that form HJs, and in red we show the systems that did not survive the EKL process. The solid line represents the analytical prediction for the first flip (see the text). The different runs we considered are labeled in the figure.

(A color version of this figure is available in the online journal.)

spin–orbit angle distribution and the overall *rate* of HJ formation. Here, we examine these questions for HJs produced via the EKL mechanism and Kozai capture.

The efficiency of HJ formation from the EKL mechanism for close ($a_2 \lesssim 500$ AU) binary systems is lower for more distant perturbers, in accordance with observations (e.g., Eggenberger et al. 2011). The formation efficiency for wide binaries is almost independent of both SMA and eccentricity for the outer orbit (see Figure 1). Following Wu et al. (2007), we estimate the fraction of stars with HJs as

$$f = f_b f_p f_{\rm EKL}, \quad (3)$$

where f_b is the fraction of stars in binary systems, f_p is the fraction of stars with Jupiter-mass planets formed at a few AU, and $f_{\rm EKL} \simeq 0.15$ is the efficiency of our mechanism from simulations. Taking $f_b \simeq 0.3$, estimated from the tail of the distribution in Duquennoy & Mayor (1991), and $f_p \simeq 0.07$,

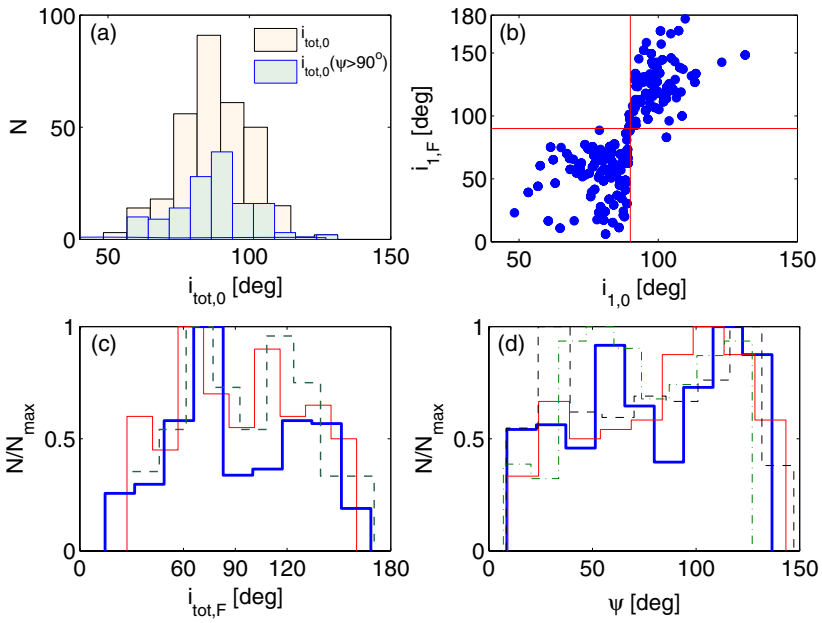

Figure 3. Effect of initial conditions on the final state for HJs formed in the SMARan run. In panel (a) we show the distribution of the initial mutual inclination ($i_{\rm tot}$) for the systems that formed HJs. We also show in light colors the initial mutual inclination for those HJs that ended up in retrograde spin–orbit configuration (i.e., $\psi > 90^\circ$). In panel (b) we show a scatter plot of the initial, $i_{1,0}$, and final, $i_{1,F}$, inner inclinations for the SMARan run. Panel (c) shows the distribution of the *final* mutual inclination for the SMARan run (thick solid blue line); we also show the distribution of the final mutual inclination for the SMA500 and SMA1000 runs (thin solid red and dashed black lines, respectively) as a function of the initial $i_{\rm tot,0}$. Panel (d) shows the distribution of the final spin–orbit angle, ψ, for the SMARan run (thick solid blue line). We also show the distribution of the final ψ for the SMA500, SMA1000, and SMA500L runs (thin solid red, dashed black, and dot-dashed green lines, respectively).

(A color version of this figure is available in the online journal.)

consistent with the studies from Wright et al. (2012) and Marcy et al. (2005), we find $f \simeq 0.0032$. The fraction of stars hosting HJs is about 1%, so we estimate that our mechanism can provide ∼30% of the total HJ formation.

Figure 4 shows the observed *projected* spin–orbit angle distribution, the distribution produced by our mechanism, and the distribution produced by the dynamical planet–planet scattering considered in Nagasawa & Ida (2011).[5] It is clear that no one mechanism is a good fit to the observed distribution: more systems are observed to be aligned than are produced by any of the proposed formation mechanisms. Aligned systems are a more natural consequence of disk migration (Lin & Papaloizou 1986; Masset & Papaloizou 2003). Following Morton & Johnson (2011; see also Fabrycky & Winn 2009), we express the complete spin–orbit angle distribution as a sum of contributions from an aligned component, an EKL component, and a dynamical planet–planet scattering component (Nagasawa & Ida 2011):

$$p(\lambda|\{f_i\}) = (1 - f_{\rm EKL} - f_{\rm scattering})\delta(\lambda) + f_{\rm EKL}\, p_{\rm EKL}(\lambda) + f_{\rm scattering}\, p_{\rm scattering}(\lambda), \quad (4)$$

with δ the Dirac delta function and $p_{\rm EKL}(\lambda)$ and $p_{\rm scattering}(\lambda)$ the distributions shown in Figure 4. The f_i represent the relative contribution of each component to the total distribution. We impose uniform priors on the f_i with $f_i \geqslant 0$ and $\sum_i f_i \leqslant 1$, and compute the posterior probability of the set of f_i, $\{f_i\}$, given the observed spin–orbit alignments (and associated errors) of 45 systems[6] from Wright et al. (2011), d, using Bayes rule:

$$p(\{f_i\}|d) \propto p(d|\{f_i\})\, p(\{f_i\}). \quad (5)$$

Treating each spin–orbit angle measurement as a Gaussian with errors given by Wright et al. (2011), the likelihood for the data set, d, is given by

$$p(d|\{f_i\}) = \prod_{i=1}^{45} \int d\lambda\, N\left(\lambda; \lambda_i, \sigma_i^\lambda\right) p(\lambda|\{f_i\}), \quad (6)$$

where the λ_i are the observed angles, σ_i^λ the observational errors, and $N(x;\mu,\sigma)$ is the Gaussian PDF with mean μ and standard deviation σ evaluated at x. The integral is evaluated over the range $\lambda \in [0, \pi]$, properly accounting for wrapping at the endpoints. The resulting probability distributions[7] for the fractional contribution of each component (aligned, EKL, and planet–planet scattering) appear in Figure 4. We also show in Figure 4 the probability distribution for the EKL contribution to the misaligned systems,

$$f_{\rm EKL}^{\rm misaligned} \equiv \frac{f_{\rm EKL}}{f_{\rm EKL} + f_{\rm scattering}}. \quad (7)$$

As expected from the distributions in Figure 4, the data support a significant aligned component, accounting for about 50% of the observed systems. The posterior is nearly degenerate along the line $f_{\rm scattering} + f_{\rm EKL} \simeq 0.5$, corresponding to a total contribution from scattering and EKL of 50%. However, the data do prefer a larger contribution from EKL than scattering, with EKL most likely accounting for ≃30% of the observed systems and planet–planet scattering ≃10% to 20% of the systems. The data prefer that EKL produces between 60% and 80% of the misaligned systems, but fractions as low as 0% and as high as 100% cannot be ruled out. Note that the allowed contribution

[5] See also the recent calculations by Boley et al. (2012) and Beauge & Nesvorny (2012).

[6] The spin–orbit observations reported at http://exoplanets.org (Wright et al. 2011).

[7] This analysis was performed using customized code implementing the algorithm described in Foreman-Mackey et al. (2012), and references therein.

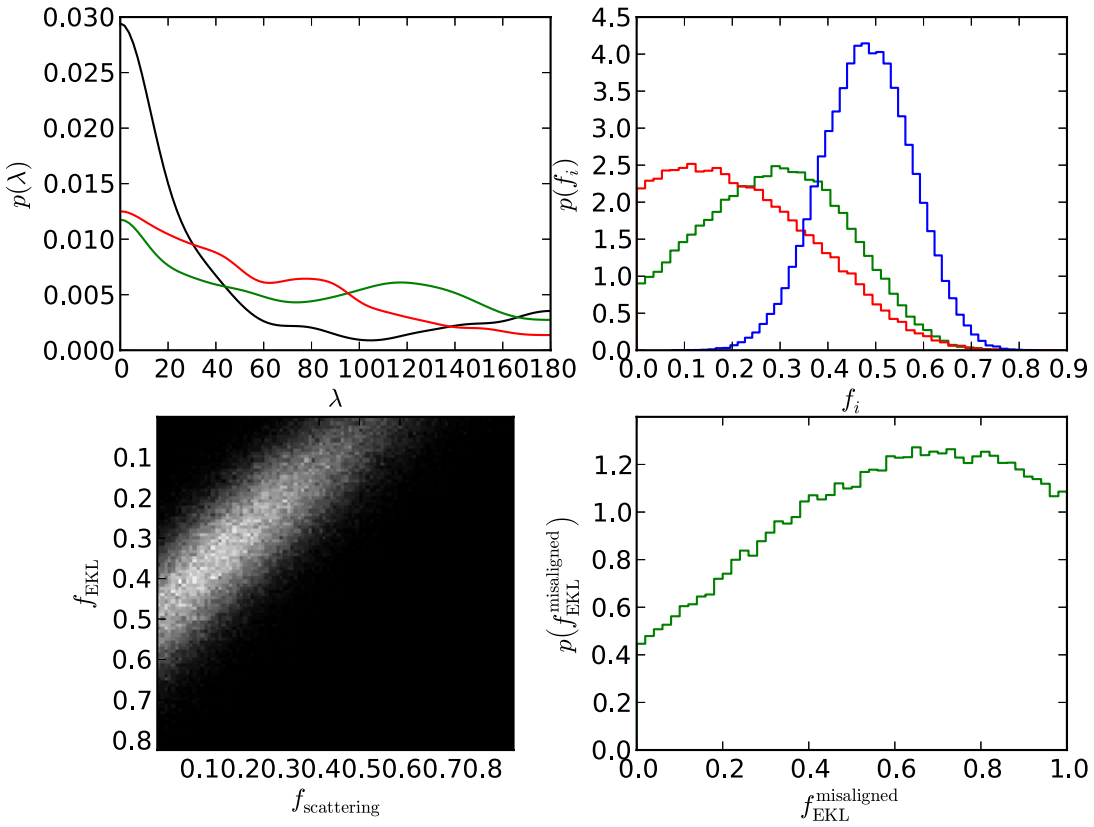

Figure 4. Upper left: distributions of projected (i.e., observed) spin–orbit angle, λ: in black, the observed distribution of spin–orbit angles in the 45 systems of Wright et al. (2011; the distribution has been smoothed using a Gaussian kernel that appropriately takes into account the observational errors in each system); in green, the distribution of spin–orbit angles produced by the EKL mechanism discussed in this work; and in red, the distribution of spin–orbit angles produced by the planet–planet scattering simulations in Nagasawa & Ida (2011). Upper right: posterior distributions of the fractional contribution of the various components to the overall spin–orbit angle distribution implied by the data (see Equations (4) and (5)); in green, distribution of the fraction of the spin–orbit distribution due to the EKL mechanism ($f_{\rm EKL}$) implied by the data; in red the distribution of the fraction due to planet–planet scattering ($f_{\rm scattering}$; Nagasawa & Ida 2011); and in blue the fraction attributed to disk migration ($1 - f_{\rm EKL} - f_{\rm scattering}$). Lower left: posterior probability distribution in the $f_{\rm scattering}$–$f_{\rm EKL}$ plane. Lower right: probability distribution for the fraction of misaligned systems produced by EKL (see Equation (7)).

(A color version of this figure is available in the online journal.)

from EKL to the shape of the spin–orbit angle distribution is consistent with the estimate from the rate of HJ production that EKL can account for about 30% of all HJ systems. Note that our calculations here ignore any processes that may re-align the spin–orbit angle after HJ formation (Albrecht et al. 2012), and thus provide a lower limit on the contributions of EKL and scattering.

Previous studies (Fabrycky & Tremaine 2007) of the secular effects of stellar perturbers have considered only the quadrupole terms in the secular potential. The expansion up to octupole order used in our work produces qualitatively different behavior. The additional terms in the potential can drive the inner orbit to much more extreme eccentricities and inclinations (including retrograde inclinations, with $i_{\rm tot} > 90^\circ$, which are impossible in the quadrupole limit), produce a flatter distribution of the spin–orbit angle, and lead to much more efficient HJ formation than found in Fabrycky & Tremaine (2007).

5. SUMMARY AND DISCUSSION

We studied the formation and evolution of HJs in wide stellar binaries using an approximation accurate to octupole order in the SMA ratio. Recent studies have shown that octuple-level perturbations can play a very important role in the dynamics of three-body systems (Naoz et al. 2011b). Naoz et al. (2011a) showed that in the presence of a second planetary-mass perturber, secular perturbations can easily produce retrograde orbits.

From an observational point of view, statistical analyses suggest that at least ∼20% of the known extrasolar planetary systems are associated with one or more stellar companions (Raghavan et al. 2006; Desidera & Barbieri 2007; Eggenberger et al. 2007), and thus stellar perturbers are likely to be at least as important as planetary perturbers.

Our results differ from those of previous studies (Fabrycky & Tremaine 2007; Wu et al. 2007) conducted at quadrupole order. We have found that the EKL mechanism produces HJs through Kozai capture about 15% of the time. Given realistic assumptions about the rate of binary stellar systems and the fraction of systems that initially host planets, we find that our mechanism can produce HJs in about 0.3% of stars. Since about 1% of stars host a HJ, EKL may account for about 30% of all HJs.

By comparing the shape of the sky-projected spin–orbit angle distribution produced by EKL, dynamical planet–planet scattering (Nagasawa & Ida 2011), and disk migration, to the observed spin–orbit angle distribution, we find that EKL likely contributes to about 30% of the observed distribution, consistent with the overall rate of HJ production.

This research was supported in part by NASA grant NNX12AI86G, and through the computational resources and

staff contributions provided by Information Technology at Northwestern University as part of its shared cluster program, Quest. We thank Yoram Lithwick, Josh Winn, John Johnson, Dan Fabrycky, Amaury Triaud, and Simon Albrecht. This research made use of the Exoplanet Orbit Database and the Exoplanet Data Explorer at exoplanets.org.

REFERENCES

Albrecht, S., Winn, J. N., Johnson, J. A., et al. 2012, arXiv:1206.6105
Beauge, C., & Nesvorny, D. 2012, ApJ, 751, 119
Boley, A. C., Payne, M. J., Corder, S., et al. 2012, ApJ, 750, L21
Correia, A. C. M., Laskar, J., Farago, F., & Boué, G. 2011, Celest. Mech. Dyn. Astron., 111, 105
Desidera, S., & Barbieri, M. 2007, A&A, 462, 345
Duquennoy, A., & Mayor, M. 1991, A&A, 248, 485
Eggenberger, A., Udry, S., Chauvin, G., et al. 2007, A&A, 474, 273
Eggenberger, A., Udry, S., Chauvin, G., et al. 2011, in IAU Symp. 276, The Astrophysics of Planetary Systems: Formation, Structure, and Dynamical Evolution, ed. A. Sozzetti, M. G. Lattanzi, & A. P. Boss (Cambridge: Cambridge Univ. Press), 409
Eggleton, P. P., Kiseleva, L. G., & Hut, P. 1998, ApJ, 499, 853
Eggleton, P. P., & Kiseleva-Eggleton, L. 2001, ApJ, 562, 1012
Fabrycky, D., & Tremaine, S. 2007, ApJ, 669, 1298
Fabrycky, D. C., & Winn, J. N. 2009, ApJ, 696, 1230
Foreman-Mackey, D., Hogg, D. W., Lang, D., & Goodman, J. 2012, arXiv:1202.3665
Gaudi, B. S., & Winn, J. N. 2007, ApJ, 655, 550
Goldreich, P., & Soter, S. 1966, Icarus, 5, 375
Holman, M., Touma, J., & Tremaine, S. 1997, Nature, 386, 254
Innanen, K. A. 1980, AJ, 85, 81
Katz, B., Dong, S., & Malhotra, R. 2011, Phys. Rev. Lett., 107, 181101
Kozai, Y. 1962, AJ, 67, 591
Kratter, K. M., & Perets, H. B. 2012, ApJ, 753, 91
Lai, D., Foucart, F., & Lin, D. N. C. 2011, MNRAS, 412, 2790
Lidov, M. L. 1962, Planet. Space Sci., 9, 719
Lin, D. N. C., & Papaloizou, J. 1986, ApJ, 309, 846
Lithwick, Y., & Naoz, S. 2011, ApJ, 742, 94
Marcy, G., Butler, R. P., Fischer, D., et al. 2005, Prog. Theor. Phys. Suppl., 158, 24
Mardling, R. A., & Aarseth, S. J. 2001, MNRAS, 321, 398
Masset, F. S., & Papaloizou, J. C. B. 2003, ApJ, 588, 494
Matsumura, S., Peale, S. J., & Rasio, F. A. 2010, ApJ, 725, 1995
Moorhead, A. V., Ford, E. B., Morehead, R. C., et al. 2011, ApJS, 197, 1
Morais, M. H. M., & Giuppone, C. A. 2012, MNRAS, 424, 52
Morton, T. D., & Johnson, J. A. 2011, ApJ, 729, 138
Mugrauer, M., & Neuhäuser, R. 2009, A&A, 494, 373
Nagasawa, M., & Ida, S. 2011, ApJ, 742, 72
Naoz, S., Farr, W. M., Lithwick, Y., Rasio, F. A., & Teyssandier, J. 2011a, Nature, 473, 187
Naoz, S., Farr, W. M., Lithwick, Y., Rasio, F. A., & Teyssandier, J. 2011b, arXiv:1107.2414
Nutzman, P. A., Fabrycky, D. C., & Fortney, J. J. 2011, ApJ, 740, L10
Raghavan, D., Henry, T. J., Mason, B. D., et al. 2006, ApJ, 646, 523
Raghavan, D., McAlister, H. A., Henry, T. J., et al. 2010, ApJS, 190, 1
Sanchis-Ojeda, R., & Winn, J. N. 2011, ApJ, 743, 61
Shporer, A., Brown, T., Mazeh, T., & Zucker, S. 2012, Nature, 17, 309
Takeda, G., Kita, R., & Rasio, F. A. 2008, ApJ, 683, 1063
Thies, I., Kroupa, P., Goodwin, S. P., Stamatellos, D., & Whitworth, A. P. 2011, MNRAS, 417, 1817
Triaud, A. H. M. J., Collier, C. A., Queloz, D., et al. 2010, A&A, 524, A25
Udry, S., & Santos, N. C. 2007, ARA&A, 45, 397
Veras, D., & Tout, C. A. 2012, MNRAS, 422, 1648
Wright, J. T., Fakhouri, O., Marcy, G. W., et al. 2011, PASP, 123, 412
Wright, J. T., Marcy, G. W., Howard, A. W., et al. 2012, ApJ, 753, 160
Wu, Y., & Murray, N. 2003, ApJ, 589, 605
Wu, Y., Murray, N. W., & Ramsahai, J. M. 2007, ApJ, 670, 820
Zucker, S., & Mazeh, T. 2002, ApJ, 568, L113